
**Microbeam analysis — Analytical
electron microscopy — Method for the
determination of energy resolution
for electron energy loss spectrum
analysis**

*Analyse par microfaisceaux — Microscopie électronique analytique
— Méthode de détermination de la résolution énergétique pour
l'analyse spectrale de la perte d'énergie des électrons*

STANDARDSISO.COM : Click to view the full PDF of ISO 23420:2021



STANDARDSISO.COM : Click to view the full PDF of ISO 23420:2021



COPYRIGHT PROTECTED DOCUMENT

© ISO 2021

All rights reserved. Unless otherwise specified, or required in the context of its implementation, no part of this publication may be reproduced or utilized otherwise in any form or by any means, electronic or mechanical, including photocopying, or posting on the internet or an intranet, without prior written permission. Permission can be requested from either ISO at the address below or ISO's member body in the country of the requester.

ISO copyright office
CP 401 • Ch. de Blandonnet 8
CH-1214 Vernier, Geneva
Phone: +41 22 749 01 11
Email: copyright@iso.org
Website: www.iso.org

Published in Switzerland

Contents

Page

Foreword	iv
Introduction	v
1 Scope	1
2 Normative references	1
3 Terms and definitions	1
4 Symbols and abbreviated terms	3
5 Definition of the energy resolution	5
6 Reference materials and energy determination	5
6.1 General	5
6.2 Materials selection for energy scale calibration	5
6.3 Binding energy measurement of graphite in the XPS	6
7 Measurement procedure and energy resolution determination	6
7.1 General	6
7.2 Predetermination of binding energy	8
7.2.1 Obtain graphite and the other reference sample	8
7.2.2 Measure C1s of graphite by using the XPS	8
7.3 Setup of the S/TEM and the EELS, and sample setting	8
7.4 First energy step, δE_1 , calibration	8
7.4.1 EELS acquisition set-up	8
7.4.2 Determining the EELS first energy step, δE_1	8
7.4.3 Acquisition of carbon K-edge EEL spectrum	9
7.4.4 Calculate calibrated energy step δE_{1C}	9
7.5 Measurement of peak close to the zero-loss peak, E_{CZLP} , for the other reference sample using energy step δE_1	12
7.5.1 EEL spectrum acquisition of the second reference sample using energy step δE_1	12
7.5.2 Obtain the value for CH_2 between the zero-loss peak and the peak E_{CZLP}	13
7.5.3 Calculate the peak E_{CZLP} energy	13
7.6 Second energy step, δE_2 , calibration	14
7.6.1 Determining the EELS second energy step, δE_2	14
7.6.2 Acquire E_{CZLP} EEL spectrum	15
7.6.3 Obtain the value for CH_3 between the zero-loss peak and peak E_{CZLP}	15
7.6.4 Calculate calibrated energy step δE_{2C}	15
7.7 Determining the calibrated EEL spectrometer energy resolution, ΔE	15
7.7.1 Acquisition of a ZLP EEL spectrum	15
7.7.2 Obtain the value for CH_4 for the zero-loss peak	15
7.7.3 Calculate EEL spectrometer energy resolution, ΔE	15
7.8 Record items	16
8 Uncertainty for the measurement result of energy resolution	17
Annex A (informative) Example of measurement procedure for energy resolution determination	18
Annex B (informative) Correspondence between energy values of XPS C1s and EELS carbon K edge	26
Bibliography	28

Foreword

ISO (the International Organization for Standardization) is a worldwide federation of national standards bodies (ISO member bodies). The work of preparing International Standards is normally carried out through ISO technical committees. Each member body interested in a subject for which a technical committee has been established has the right to be represented on that committee. International organizations, governmental and non-governmental, in liaison with ISO, also take part in the work. ISO collaborates closely with the International Electrotechnical Commission (IEC) on all matters of electrotechnical standardization.

The procedures used to develop this document and those intended for its further maintenance are described in the ISO/IEC Directives, Part 1. In particular, the different approval criteria needed for the different types of ISO documents should be noted. This document was drafted in accordance with the editorial rules of the ISO/IEC Directives, Part 2 (see www.iso.org/directives).

Attention is drawn to the possibility that some of the elements of this document may be the subject of patent rights. ISO shall not be held responsible for identifying any or all such patent rights. Details of any patent rights identified during the development of the document will be in the Introduction and/or on the ISO list of patent declarations received (see www.iso.org/patents).

Any trade name used in this document is information given for the convenience of users and does not constitute an endorsement.

For an explanation of the voluntary nature of standards, the meaning of ISO specific terms and expressions related to conformity assessment, as well as information about ISO's adherence to the World Trade Organization (WTO) principles in the Technical Barriers to Trade (TBT), see www.iso.org/iso/foreword.html.

This document was prepared by Technical Committee ISO/TC 202, *Microbeam analysis*, Subcommittee SC 3, *Analytical electron microscopy*.

A list of all parts in the ISO 23420 series can be found on the ISO website.

Any feedback or questions on this document should be directed to the user's national standards body. A complete listing of these bodies can be found at www.iso.org/members.html.

Introduction

In order to understand the chemical composition, the atomic bonding and the electronic structure, electron energy loss analysis is often performed with the scanning transmission electron microscope or the transmission electron microscope (S/TEM) equipped with the electron energy loss (EEL) spectrometer.

In the analysis using EEL spectrometer system, the energy loss of incident electrons by the inelastic interaction via phonon and plasmon excitations, intra- and inter-band transitions and the inner shell ionization can be measured. The inner shell ionization is particularly useful and important as it gives the information on chemical composition of materials. For the precise analysis based on the energy loss peak decomposition and its energy shifts, it is vitally important to understand the energy resolution of the EEL spectrometer system. However, the determination method of the energy resolution is not standardized yet.

This document provides the procedures for energy step calibration and energy resolution determination useful for the electron energy loss spectrum analysis in the S/TEM equipped with the EEL spectrometer.

STANDARDSISO.COM : Click to view the full PDF of ISO 23420:2021

[STANDARDSISO.COM](https://standardsiso.com) : Click to view the full PDF of ISO 23420:2021

Microbeam analysis — Analytical electron microscopy — Method for the determination of energy resolution for electron energy loss spectrum analysis

1 Scope

This document specifies a determination procedure of energy resolution in the scanning transmission electron microscope or the transmission electron microscope equipped with the electron energy loss (EEL) spectrometer.

This document is applicable to both in-column type EEL spectrometer and post-column type EEL spectrometer. These EEL signal detecting systems are applicable to a parallel detecting system and a serial detecting system.

2 Normative references

There are no normative references in this document.

3 Terms and definitions

For the purposes of this document, the following terms and definitions apply.

ISO and IEC maintain terminological databases for use in standardization at the following addresses:

- IEC Electropedia: available at <http://www.electropedia.org/>
- ISO Online browsing platform: available at <https://www.iso.org/obp>

3.1

beam diameter

full width at half maximum (FWHM) of the electron beam intensity profile for the STEM observation

3.2

Boersch effect

energy spread of electron beam due to *Coulomb interaction* (3.5) between electrons in the beam

3.3

channel

range of one pixel of the detector in the *parallel detection* (3.17) EELS

3.4

collection angle

EELS entrance aperture diameter divided by a camera length and a *geometric factor* (3.13) for the STEM or the TEM diffraction mode, or EELS entrance aperture diameter divided by the distance from crossover of the lens in front of the EEL spectrometer to the EELS entrance aperture for imaging mode of the energy-filtering TEM

3.5

Coulomb interaction

repulsion of electrons by electric charge

3.6

detection plane

plane where energy dispersed electron focus

3.7

electron energy loss

energy shift of the electron kinetic energy due to the inelastic scattering in solids

3.8

energy dispersion

degree of change in position of the dispersed electrons at the *detection plane* (3.6) per unit energy change

3.9

energy resolution

FWHM of the *zero-loss* (3.21) peak

3.10

energy step

energy selecting window (3.11) per *channel* (3.3) in the *parallel detection* (3.17) EELS, or energy range limited by the width of energy selecting slit in the *serial detection* (3.20) EELS

3.11

energy selecting window

energy range for selection of a specific energy loss value

3.12

entrance aperture

aperture for limiting the *collection angle* (3.4) of the EEL spectrometer

3.13

geometric factor

ratio of distance from a projector lens to an EELS entrance aperture to distance from the projector lens to an image detection device

3.14

in-column type EELS

EELS system with the EEL spectrometer located in the imaging system of the TEM

3.15

irradiation diameter

diameter of the electron beam irradiation region for the TEM observation

3.16

K edge

energy loss related to K shell electron transition to the lowest empty state

3.17

parallel detection

simultaneous EELS signal detection for all energy-dispersed electrons focused on the *detection plane* (3.6)

3.18

plasmon-loss

energy loss of electron due to excitation of the quantized plasma oscillations of electrons

3.19

post-column type EELS

EELS system with the EEL spectrometer located behind the imaging/detecting system of the TEM

3.20

serial detection

EEL spectrum detection by scanning the dispersed electrons across the energy selecting slit in front of the detector

3.21

zero-loss

unscattered and elastically scattered electrons (with only minimal loss of energy due to phonon excitation), giving rise to an intensity peak or the position of which defines zero in the electron energy loss spectrum

[SOURCE: ISO15932: 2013, 2.2.1.1]

4 Symbols and abbreviated terms

<i>B</i>	spatial width of energy selecting window in the serial detection of the EELS
CCD	charge coupled device
CFE	cold field emission
CH_1	sum of $Ch_1(G, P)$ and the $Ch_1(G, C-K)$. In the parallel detection system, CH_1 is the number of channels between the zero-loss peak and carbon K edge of graphite. In the serial detection system, CH_1 is distance between the zero-loss peak and carbon K edge of graphite.
CH_2	number of channels between the zero-loss peak [Figure 5, key 1] and the peak E_{CZLP} [Figure 5, key 2] on the calibrated energy step δE_{1C} in the parallel detection EELS. In the serial detection EELS, CH_2 is distance between the zero-loss peak [Figure 5, key 1] and the peak E_{CZLP} [Figure 5, key 2] on the calibrated energy step δE_{1C} .
CH_3	number of channels between the zero-loss peak and the peak E_{CZLP} on the energy step δE_2 in the parallel detection EELS. In the serial detection EELS, CH_3 is distance between the zero-loss peak and the peak E_{CZLP} on the energy step δE_2 .
CH_4	number of channels corresponding to FWHM of the zero-loss peak on the calibrated energy step δE_{2C} in the parallel detection EELS. In the serial detection EELS, CH_4 is distance between the zero-loss peak and the peak E_{CZLP} on the calibrated energy step δE_{2C} .
$Ch_1(G, C-K)$	number of channels of the range from the graphite plasmon-loss ($\pi + \sigma$) peak [Figure 3, key 1] to carbon K edge E_{C-K} [Figure 3, key 2] on the energy step δE_1 in the parallel detection system. In the serial detection system, $Ch_1(G, C-K)$ is distance between the graphite plasmon-loss ($\pi + \sigma$) peak [Figure 3, key 1] and carbon K edge E_{C-K} [Figure 3, key 2] on the energy step δE_1 .
$Ch_1(G, P)$	number of channels of the range from the zero-loss peak [Figure 2, key 1] to the graphite plasmon-loss ($\pi + \sigma$) peak E_{CZLP} [Figure 2, key 2] on the energy step δE_1 in the parallel detection system. In the serial detection system, $Ch_1(G, P)$ is distance between the zero-loss peak [Figure 2, key 1] and the graphite plasmon-loss ($\pi + \sigma$) peak E_{CZLP} [Figure 2, key 2] on the energy step δE_1 .
CMOS	complementary metal oxide semiconductor
CRM	certified reference material
C1s	carbon K shell binding energy of graphite measured by the XPS
<i>D</i>	energy dispersion on the recording device of the EEL spectrometer
<i>d</i>	sample thickness of the electron beam irradiated area
<i>E</i>	value of electron energy loss such as plasmon-loss and ionization-loss
E_{BN-P}	measured plasmon-loss ($\pi - \pi^*$) peak energy of boron-nitride under the condition of calibrated energy step δE_{1C}

E_{CZLP}	position of noticed low-loss peak close to the zero-loss peak
$E_{\text{C-K}}$	carbon K edge energy in the EELS
EEL	electron energy loss
EELS	electron energy loss spectroscope/spectroscopy
FWHM	full width at half maximum
GUM	guide to the expression of uncertainty in measurement
m	total number of available channels in the parallel detection of the EELS
n	iteration number in acquisition of electron energy loss spectrum
RM	reference material
STEM	scanning transmission electron microscope/microscopy
S/TEM	scanning transmission electron microscope/microscopy or transmission electron microscope/microscopy
s	detector spatial resolution for the parallel detection. For the serial detection, s is slit width of energy selecting window
TEM	transmission electron microscope/microscopy
t	acquisition time in acquisition of electron energy loss spectrum
XPS	X-ray photoelectron spectroscope/spectroscopy
ZLP	zero-loss peak
ΔE	energy resolution
ΔE_{r}	theoretical energy resolution
ΔE_{S0}	energy broadening
δE_1	selected energy step in the first energy calibration. In the parallel detection system, δE_1 is selected from the preset value. In the serial detection system, δE_1 is derived from the energy width and its spatial width in the energy selection window
$\delta E_{1\text{C}}$	calibrated value of energy step δE_1
δE_2	selected energy step in the second energy calibration. In the parallel detection system, δE_2 is selected from the preset value. In the serial detection system, δE_2 is derived from the energy width and its spatial width in the energy selection window.
$\delta E_{2\text{C}}$	calibrated energy step of energy step δE_2 by the second energy calibration step
δE_{S}	energy width of the energy-selecting window in the serial detection system of the EELS
λ	mean free path of electron inelastic scattering
π	π -bonding state
π^*	π -antibonding state

σ	σ -bonding state
$(\pi - \pi^*)$	resonant oscillation of the π -bonding state and the π -antibonding state
$(\pi + \sigma)$	resonant oscillation of the π -bonding state and the σ -bonding state

5 Definition of the energy resolution

The theoretical energy resolution ΔE_r is given from a convolution of an electron beam energy spread and a spectrometer resolution. The theoretical energy resolution is shown as [Formula \(1\)](#)^[2].

$$(\Delta E_r)^2 \approx (\Delta E_0)^2 + (\Delta E_{S0})^2 + (s / D)^2 \quad (1)$$

where

ΔE_r is theoretical energy resolution

ΔE_0 is energy spread of the primary electron beam

NOTE ΔE_0 is affected by energy width of electron source and the Boersch effect.

ΔE_{S0} is broadening of energy

NOTE ΔE_{S0} is affected both the spectrometer focusing and the angular width of inelastic scattering.

s is a detector spatial resolution for the parallel detection. For the serial detection, s is a slit width of energy selecting window.

D is an energy dispersion of the spectrometer

In addition, acquisition time t and acquisition iteration number n influence the energy resolution ΔE_r .

Measurement of energy resolution ΔE_r is not easy because of the complicated formation of the EELS system. It is well known that the full width at half maximum of the zero-loss peak is proportional to the energy resolution ΔE_r . Actually, FWHM of the zero-loss peak is very often used as the energy resolution^[3]. The energy resolution ΔE is also defined as FWHM of the zero-loss peak in this document.

6 Reference materials and energy determination

6.1 General

In order to determine the energy resolution of the EELS equipped in the S/TEM, it is indispensable to calibrate the energy scale in advance. In this section, material selection for the energy scale calibration and the procedure for determining the energy scale are described.

6.2 Materials selection for energy scale calibration

For the energy resolution determination, calibration of the energy scale is necessary. As an EEL spectrometer cannot calibrate energy scale by itself, the reference material is necessary for the calibration. Since the energy calibrated certified reference materials (CRMs) and/or reference materials (RMs) are not available, it is necessary to select appropriate materials aiming to energy scale calibration, as (internal) reference materials. The following characteristics are required for the material.

- Easy to obtain
- Easy to handle,

- Homogeneous,
- Stable,
- Having loss peaks at a low-loss energy region,

NOTE 1 For measuring the energy resolution, energy scale calibration is needed to perform within loss energy region such as zero to several hundred electronvolt.

- Non-chargeable.

NOTE 2 In the first step of energy scale calibration on the EELS, loss energy known sample is needed. The loss energy value is obtained by the XPS analysis of the sample. Non-chargeable material is needed for XPS measurements.

In this document, graphite is recommended and used as a reference sample for the coarse energy scale calibration. The other reference sample for the following fine energy scale calibration should be selected from the materials, which has low-loss EELS peak, such as boron-nitride.

6.3 Binding energy measurement of graphite in the XPS

XPS C1s (carbon K shell binding energy) peak and EELS carbon K edge E_{C-K} are equivalent. The correspondence of the energy values between XPS C1s and EELS carbon K-edge is described in [Annex B](#). XPS measurement of C1s peak shall be done about graphite standard sample with calibrated XPS spectrometer.

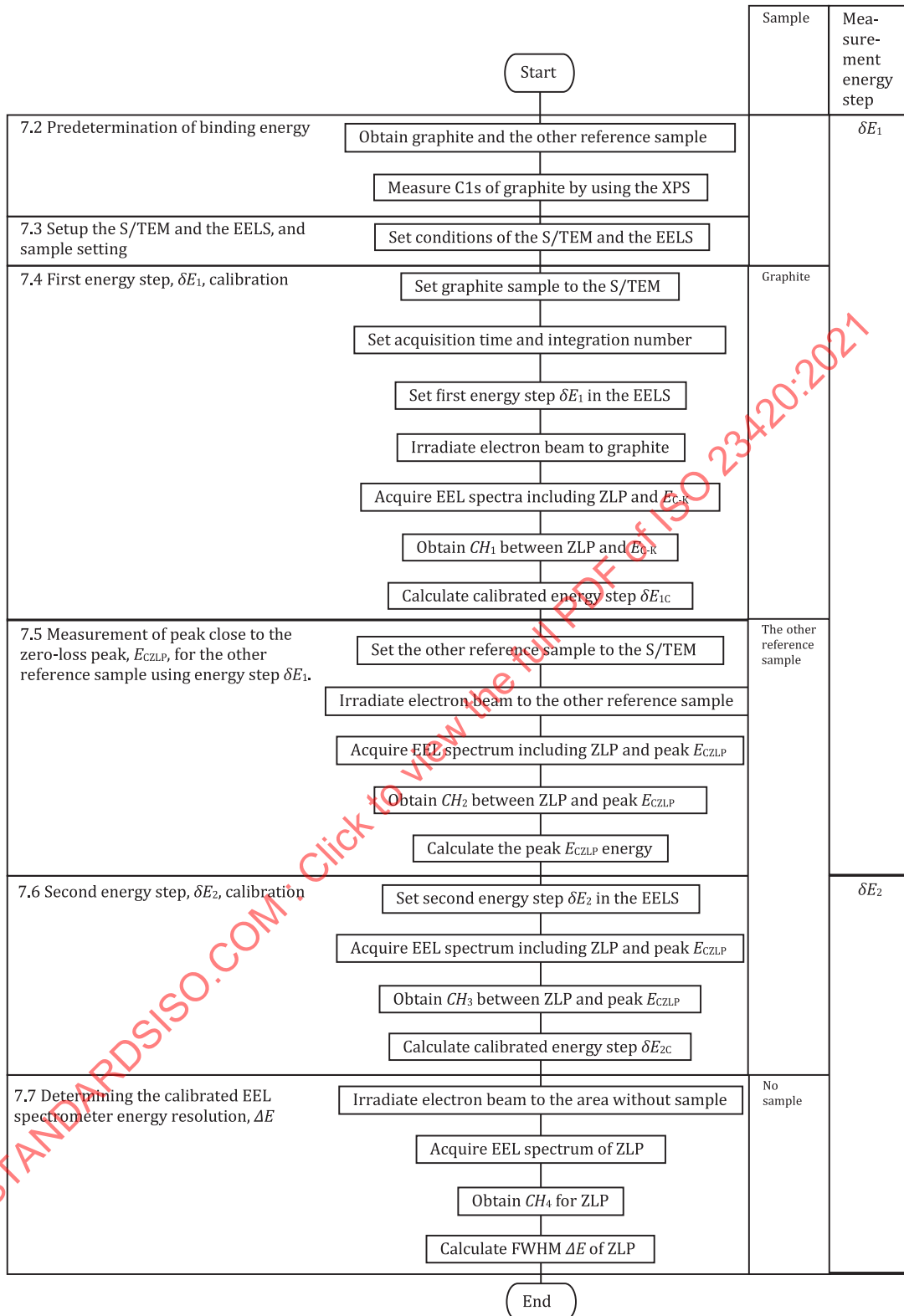
The XPS shall be calibrated by ISO 15472:2010^[4].

7 Measurement procedure and energy resolution determination

7.1 General

In this subclause, the energy scale calibration of EELS and the procedure for determining energy resolution are described. [Annex A](#) shows an example of actual measurement using this procedure.

A flowchart of measurement procedure is shown in [Figure 1](#).



NOTE Numbers given in [Figure 1](#) indicate corresponding clauses in this document.

Figure 1 — Flow chart of measurement procedure

7.2 Predetermination of binding energy

7.2.1 Obtain graphite and the other reference sample

Obtain a graphite and a second reference sample. The graphite reference sample has a Carbon K-edge and an EEL peak E_{CZLP} in an EEL spectrum. The second reference sample should have an EEL peak E_{CZLP} appearing close to the zero-loss peak, but the peak spread should not overlap with the zero-loss peak. For example, the boron nitride plasmon-loss ($\pi - \pi^*$) peak is suitable for the E_{CZLP} as good as the graphite plasmon-loss ($\pi + \sigma$) peak.

7.2.2 Measure C1s of graphite by using the XPS

Measure the carbon K-shell binding energy of the graphite using XPS. The C1s is used as carbon K edge energy E_{C-K} of graphite of the EELS. The XPS shall be calibrated by ISO 15472:2010.

7.3 Setup of the S/TEM and the EELS, and sample setting

Samples are recommended to be drop-cast onto a TEM grid, e.g. a holey carbon film support grid, to ease the measurement. The electron microscope should be adjusted for S/TEM observation in advance. EELS should also be adjusted in advance so that EEL spectra can be easily obtained. Parameters of the S/TEM and the EELS are recorded as described in [7.8](#).

The quality of an EEL spectrum is easily affected by electron beam induced carbon contamination. The use of an anti-contamination device is strongly recommended for suppression of the contamination. Additionally, a clean environment in the column is also needed to minimise the contamination.

7.4 First energy step, δE_1 , calibration

7.4.1 EELS acquisition set-up

Set the EEL spectrometer acquisition time and integration numbers so as to secure a sufficient signal-to-noise ratio without any peak saturation for all measurements, including measurements in subsequent sections. Since the measurement conditions such as irradiation current, entrance aperture diameter and capturing device characterization like CCD / CMOS camera are different, acquisition time and integration number cannot be uniformized. Therefore, users of this procedure should optimise acquisition time and integration number for their own systems and should record these values.

7.4.2 Determining the EELS first energy step, δE_1

Set the energy step δE_1 to cover all range from the zero-loss peak to the carbon K edge E_{C-K} of graphite.

In the parallel detection system, energy step δE_1 is selected from the preset value under the condition as [Formula \(2\)](#).

$$\delta E_1 \geq E_{C-K} / m \quad (2)$$

where

E_{C-K} is carbon K edge energy in the EELS

m is total number of available channels in the parallel detection system of the EELS

In the serial detection system, set a full measurement range as the zero-loss peak to the carbon K edge E_{C-K} of graphite. Energy step δE_1 is obtained as [Formula \(3\)](#).

$$\delta E_1 = \delta E_S / B \quad (3)$$

where

δE_S is energy width of the energy-selecting window in the serial detection system of the EELS

B is spatial width of energy selecting window in the serial detection system of the EELS

7.4.3 Acquisition of carbon K-edge EEL spectrum

Irradiate a thin region of graphite with the electron beam and acquire an EEL spectrum including the ZLP and the carbon K-shell edge. A d/λ (sample thickness / mean free path) ratio check should be performed to ensure the thickness of the area irradiated is suitable for the procedure.

Since the intensities of the zero-loss peak, the plasmon-loss ($\pi + \sigma$) peak and carbon K edge E_{C-K} are considerably different, spectra including all these peaks may need to be acquired separately.

If it is necessary to acquire separate EEL spectra, an EEL spectrum should be acquired to include the zero-loss peak and the plasmon-loss ($\pi + \sigma$) peak, this region will give the value for $Ch_1(G, P)$, ([Figure 2](#)). Acquire a 2nd spectra which includes the plasmon-loss ($\pi + \sigma$) peak and carbon K edge E_{C-K} , this region will give the value for $Ch_1(G, C-K)$, ([Figure 3](#)).

Furthermore, the sum of $Ch_1(G, P)$ and the $Ch_1(G, C-K)$ gives the value for CH_1 (see [7.4.4](#)).

Certain EELS systems are able to acquire $Ch_1(G, P)$ and $Ch_1(G, C-K)$ simultaneously if the EELS system has a function capable of obtaining two regions of the EEL spectrum.

7.4.4 Calculate calibrated energy step δE_{1C}

Obtain calibrated energy step δE_{1C} as [Formula \(4\)](#). δE_{1C} is the calibrated value of energy step δE_1 .

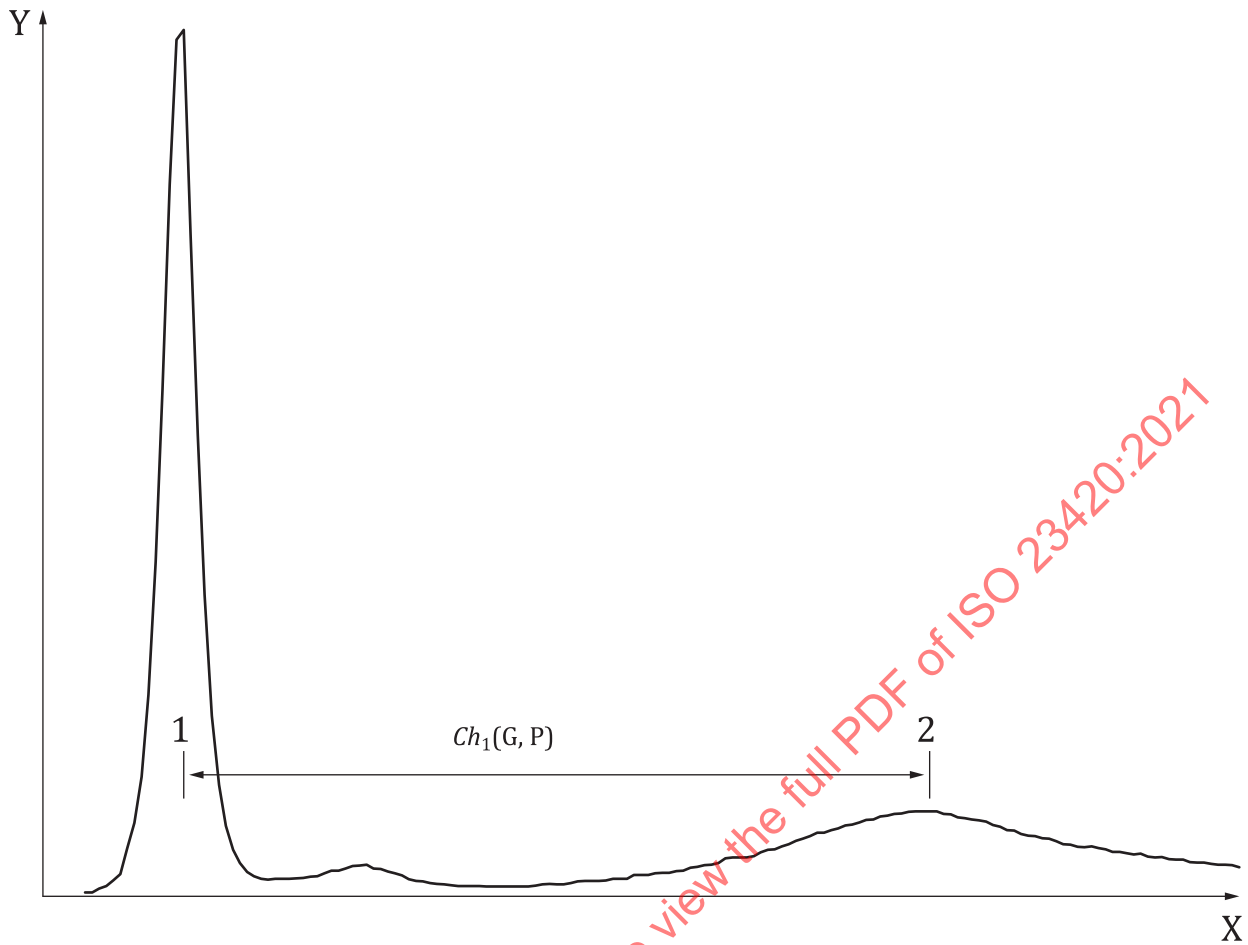
$$\delta E_{1C} = E_{C-K} / CH_1 = E_{C-K} / (Ch_1(G, P) + Ch_1(G, C-K)) \quad (4)$$

where

$Ch_1(G, P)$ is the number of channels of the range from the zero-loss peak [[Figure 2](#), key 1] to the graphite plasmon-loss ($\pi + \sigma$) peak E_{CZLP} [[Figure 2](#), key 2] on the energy step δE_1 in the parallel detection system. In the serial detection system, $Ch_1(G, P)$ is distance between the zero-loss peak [[Figure 2](#), key 1] and the graphite plasmon-loss ($\pi + \sigma$) peak E_{CZLP} [[Figure 2](#), key 2] on the energy step δE_1 .

$Ch_1(G, C-K)$ is the number of channels of the range from the graphite plasmon-loss ($\pi + \sigma$) peak [[Figure 3](#), key 1] to carbon K edge E_{C-K} [[Figure 3](#), key 2] on the energy step δE_1 in the parallel detection system. In the serial detection system, $Ch_1(G, C-K)$ is distance between the graphite plasmon-loss ($\pi + \sigma$) peak [[Figure 3](#), key 1] and carbon K edge E_{C-K} [[Figure 3](#), key 2] on the energy step δE_1 .

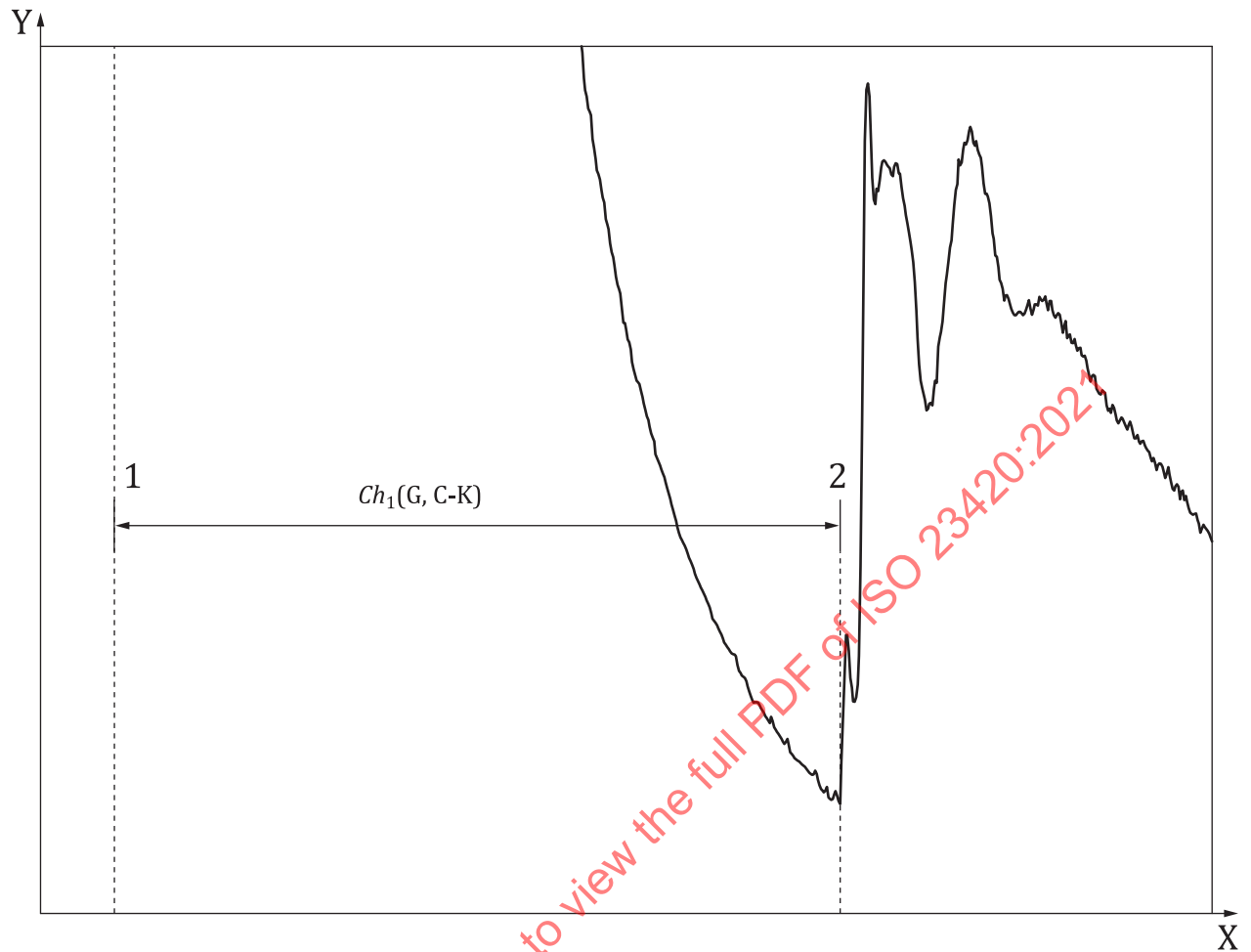
In this document, the EELS carbon K edge position corresponding to the XPS C1s peak is set to half height [[Figure 4](#), key 2] between peak [[Figure 4](#), key 1] and dip [[Figure 4](#), key 3] of a background-subtracted spectrum for EELS carbon K edge as example of [Figure 4](#).



Key

- X channel number or distance
- Y counts
- 1 zero-loss peak
- 2 plasmon-loss ($\pi + \sigma$) peak

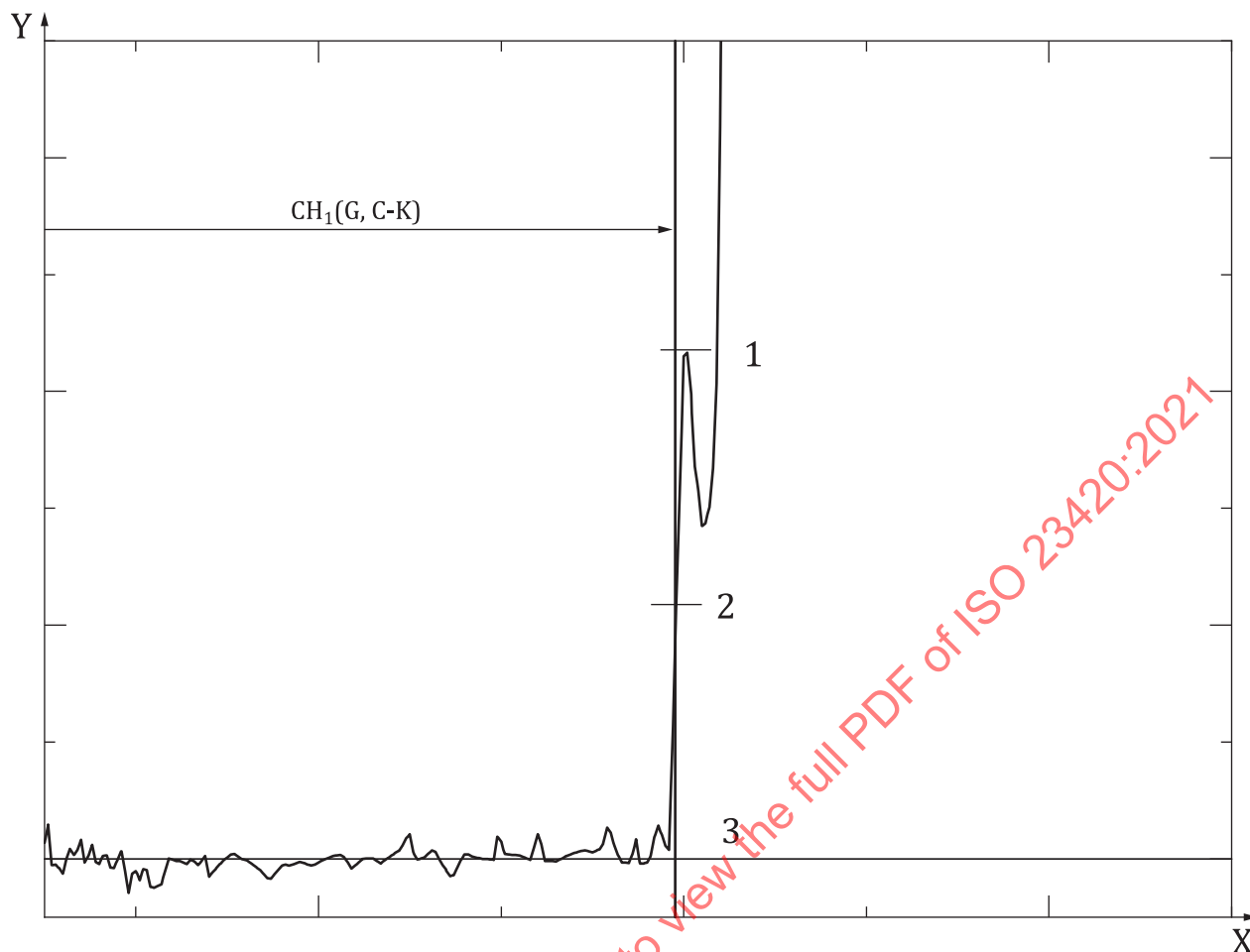
Figure 2 — EEL spectrum of the zero-loss peak and plasmon-loss ($\pi + \sigma$) peak for graphite

**Key**

- X channel number or distance
- Y counts
- 1 plasmon-loss ($\pi + \sigma$) peak
- 2 carbon K edge

NOTE This peak of the key 1 is the same as the key 2 of the [Figure 2](#).

Figure 3 — EEL spectrum of carbon K edge for graphite

**Key**

- X channel number or distance
- Y counts
- 1 peak of carbon K edge
- 2 half height of carbon K edge
- 3 dip of carbon K edge

NOTE This edge is the same as the key 2 of [Figure 3](#).

Figure 4 — Background-subtracted EEL spectrum of carbon K edge for graphite

7.5 Measurement of peak close to the zero-loss peak, E_{CZLP} , for the other reference sample using energy step δE_1

7.5.1 EEL spectrum acquisition of the second reference sample using energy step δE_1

Exchange the sample for the second reference sample and position the sample so that it is within the field of view of the S/TEM.

Irradiate the electron beam to a thin region of the sample that does not overlap with other materials. A d/λ (sample thickness / mean free path) ratio check should be performed to ensure the thickness of the area irradiated is suitable for the procedure.

Maintaining the same δE_1 , acquire an EEL spectrum including the zero-loss peak and the peak E_{CZLP} , see [Figure 5](#).

7.5.2 Obtain the value for CH_2 between the zero-loss peak and the peak E_{CZLP}

Obtain the value for CH_2 between the zero-loss peak and peak E_{CZLP} . In the parallel detection system, CH_2 is the number of channels between the zero-loss peak [Figure 5, key 1] and the peak E_{CZLP} [Figure 5, key 2] on the energy step δE_1 . In the serial detection system, CH_2 is distance between the zero-loss peak [Figure 5, key 1] and the peak E_{CZLP} [Figure 5, key 2] on the energy step δE_1 .

7.5.3 Calculate the peak E_{CZLP} energy

Obtain the peak E_{CZLP} energy as Formula (5).

$$E_{CZLP} = \delta E_{1C} \cdot CH_2 \quad (5)$$

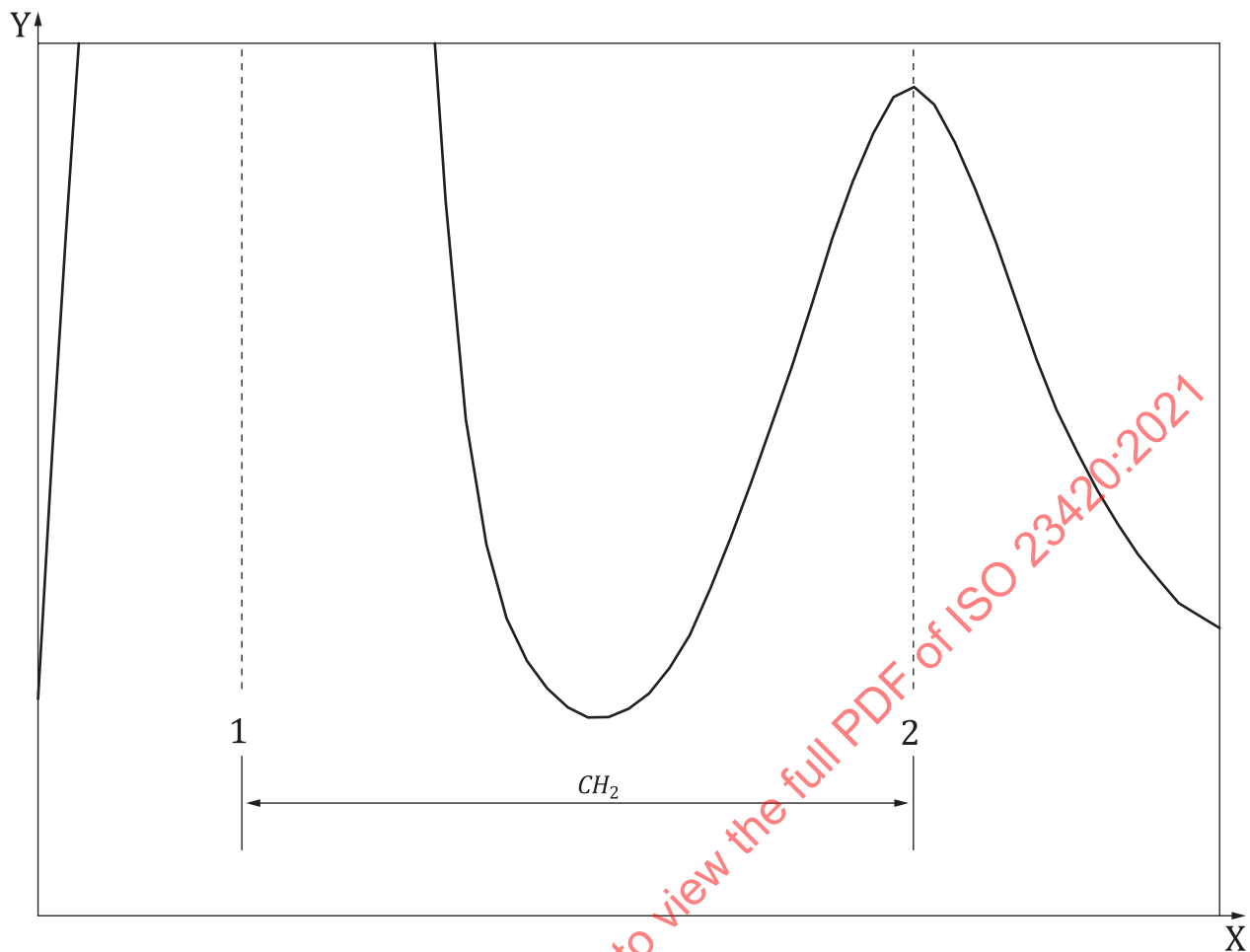
where

E_{CZLP} is the position of noticed low-loss peak close to the zero-loss peak

CH_2 is the number of channels between the zero-loss peak [Figure 5, key 1] and the peak E_{CZLP} [Figure 5, key 2] on the energy step δE_1 in the parallel detection EELS. In the serial detection EELS, CH_2 is distance between the zero-loss peak [Figure 5, key 1] and the peak E_{CZLP} [Figure 5, key 2] on the energy step δE_1

This value is used for the calibration of the fine energy step, at the next process.

STANDARDSISO.COM : Click to view the full PDF of ISO 23420:2021



Key

- X channel number or distance
- Y counts
- 1 zero-loss peak
- 2 peak E_{CZLP}

Figure 5 — EEL spectrum of the zero-loss peak and peak E_{CZLP} for the other reference sample

7.6 Second energy step, δE_2 , calibration

7.6.1 Determining the EELS second energy step, δE_2

Set the energy step δE_2 to cover all range from the zero-loss peak to peak E_{CZLP} .

In the parallel detection system, selectable energy step and simultaneous detection channel number m are predetermined. Thus, energy step δE_2 is selected under the condition as [Formula \(6\)](#).

$$\delta E_2 \geq E_{CZLP} / m \tag{6}$$

In the serial detection system, set a full measurement range as the zero-loss peak to peak E_{CZLP} . Energy step δE_2 is obtained as [Formula \(7\)](#).

$$\delta E_2 = \delta E_S / B \tag{7}$$

7.6.2 Acquire E_{CZLP} EEL spectrum

Acquire an EEL spectrum including the zero-loss peak and peak E_{CZLP} by energy step δE_2 , as per [Figure 5](#).

7.6.3 Obtain the value for CH_3 between the zero-loss peak and peak E_{CZLP}

Obtain the value for CH_3 between the zero-loss peak and peak E_{CZLP} . In the parallel detection system, CH_3 is the number of channels between the zero-loss peak and peak E_{CZLP} . In the serial detection EELS, CH_3 is distance between the zero-loss peak and peak E_{CZLP} .

7.6.4 Calculate calibrated energy step δE_{2C}

Calibrated (actual) energy step δE_{2C} is obtained by using observed peak E_{CZLP} as [Formula \(8\)](#).

$$\delta E_{2C} = E_{\text{CZLP}} / CH_3 \quad (8)$$

7.7 Determining the calibrated EEL spectrometer energy resolution, ΔE

7.7.1 Acquisition of a ZLP EEL spectrum

Irradiate electron beam to an area without the sample and acquire an EEL spectrum of the ZLP.

7.7.2 Obtain the value for CH_4 for the zero-loss peak

Obtain the value for CH_4 for the zero-loss peak.

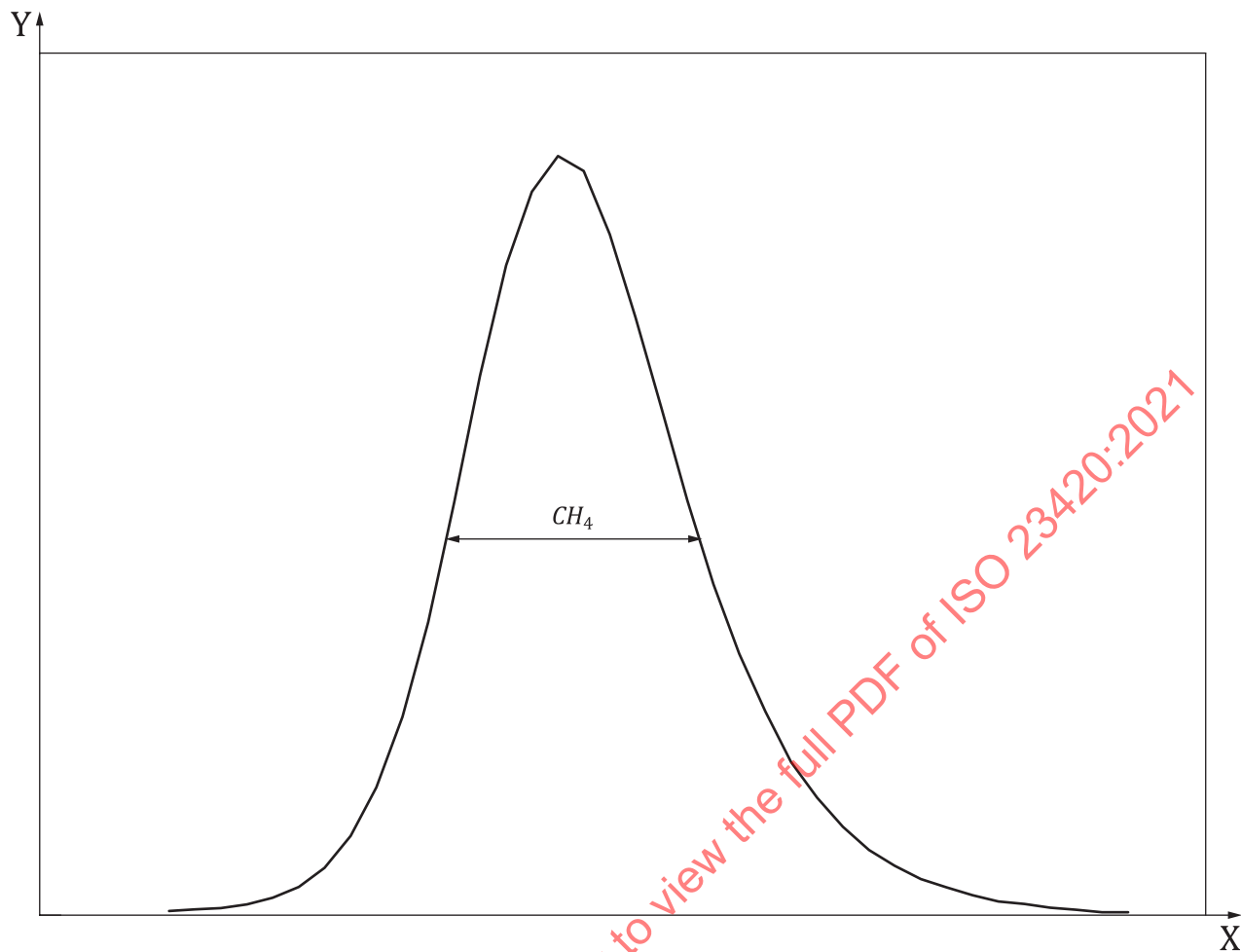
where CH_4 is the number of channels corresponding to FWHM [[Figure 6](#)] of the zero-loss peak on the energy step δE_2 in the parallel detection EELS. In the serial detection EELS, CH_4 is distance between the zero-loss peak and the peak E_{CZLP} on the energy step δE_2 .

7.7.3 Calculate EEL spectrometer energy resolution, ΔE

Use the FWHM of the zero-loss peak and δE_{2C} to determine the EEL spectrometer energy resolution, ΔE , as per [Formula \(9\)](#).

$$\Delta E = \delta E_{2C} \cdot CH_4 \quad (9)$$

where ΔE is energy resolution



Key

- X channel number or distance
- Y counts

Figure 6 — Zero-loss peak with no sample and its FWHM

7.8 Record items

These items as follows are recorded.

For the electron microscope,

- S/TEM manufacturer and model name
- Emission type of the electron gun such as cold field emission (CFE), Schottky, lanthanum hexaboride (LaB₆) cathode, tungsten (W) filament and any other emission systems
- Acceleration voltage
- With or without a monochromator for the electron beam
- Imaging / diffraction mode such as TEM, diffraction and STEM
- Information for beam diameter or irradiation diameter such as preset value, nominal number of beam diameter, etc.
- Irradiation beam current

For the EELS,

- EEL spectrometer manufacturer and model name
- Diameter of the entrance aperture
- Preset and calibrated energy step in each measurement step
- In the parallel detection system, the number of channels between interest points in each step such as zero-loss and carbon K edge
- In the serial detection system, distance between interest points in each step
- Acquisition condition such as acquisition time and integration number in each step

NOTE Set the acquisition time and integration numbers so as to secure the sufficient signal-to-noise ratio and no peak saturation for each energy measurement

8 Uncertainty for the measurement result of energy resolution

This section describes the combined uncertainty followed by the uncertainties that occur at each step of the measurement procedure. There are five uncertainty factors in the procedure. These uncertainty factors are classified types as A or B in the guide to the expression of uncertainty in measurement (GUM).^[5]

σE_{C-K} uncertainty of the carbon K shell binding energy C1s measured by the XPS calibrated with ISO 15472, classified as type B

$\sigma(\delta E_{1C})$ uncertainty of the corrected energy step δE_{1C} , classified as type A

σE_{CZLP} uncertainty of the peak energy E_{CZLP} , classified as type A

$\sigma(\delta E_{2C})$ uncertainty of the corrected energy step δE_{2C} , classified as type A

$\sigma(\Delta E)$ uncertainty of the FWHM ΔE of the zero-loss peak, classified as type A

The uncertainty $\sigma(\delta E_{1C})$, σE_{CZLP} , $\sigma(\delta E_{2C})$ and $\sigma(\Delta E)$ shall be calculated from the results by N_1 , N_2 , N_3 , and N_4 replicate measurements. To do this, the measurements shall be repeated N_1 , N_2 , N_3 , and N_4 times, respectively. The frequency of repetitions (namely N_1 , N_2 , N_3 , and N_4) shall be three times or more.

A combined standard uncertainty U_C is expressed using [Formula \(10\)](#):

$$U_C = \sqrt{(\sigma E_{C-K})^2 + \left(\frac{\sigma(\delta E_{1C})}{\sqrt{N_1}}\right)^2 + \left(\frac{\sigma E_{CZLP}}{\sqrt{N_2}}\right)^2 + \left(\frac{\sigma(\delta E_{2C})}{\sqrt{N_3}}\right)^2 + \left(\frac{\sigma(\Delta E)}{\sqrt{N_4}}\right)^2} \quad (10)$$

An expanded standard uncertainty U is expressed using [Formula \(11\)](#):

$$U = \kappa U_C \quad (11)$$

where

κ is the coverage factor.

NOTE For confidence limit of approximately 95,45 %, κ is set to 2; and for a confidence limit of approximately 99,73 %, κ is set to 3.

Annex A (informative)

Example of measurement procedure for energy resolution determination

A.1 General

In this annex, an example of measurement procedure for energy resolution determination is described^[6].

A.2 Samples

A.2.1 Graphite as first reference sample

Natural graphite from Madagascar has been used. This graphite has high purities and crystallinities.

Carbon K shell binding energy C1s of the graphite was measured as 284,5 eV by the JEOL JPS-9200 photoelectron spectrometer. The XPS has been calibrated by ISO15472:2001.

Carbon K edge E_{C-K} of EELS was defined from the XPS result as 284,5 eV.

A.2.2 Boron-nitride as the other reference sample

Boron-nitride powder from a Japanese manufacturer has been used as the other reference sample. Plasmon-loss ($\pi - \pi^*$) peak of boron-nitride was used as energy peak E_{CZLP} .

A.2.3 Sample for the S/TEM

The S/TEM sample of the graphite and the boron-nitride supported on the micro-grid (amorphous carbon) together have been used. TEM image of the sample is shown as [Figure A.1](#).

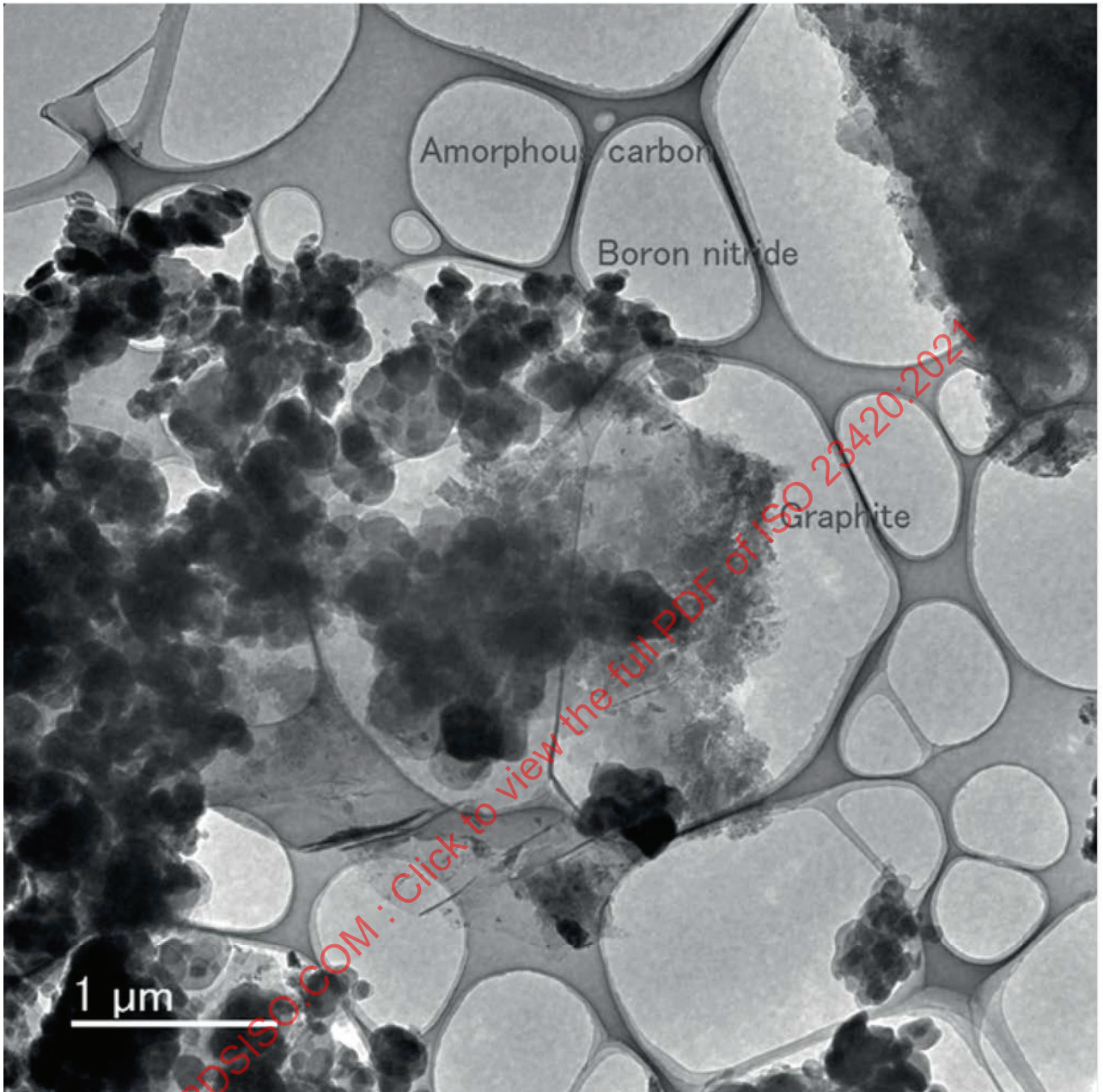


Figure A.1 — Sample TEM image

A.3 Results of example

A.3.1 Setup conditions of S/TEM

Setup conditions of the TEM are as follows.

- Model of the electron microscope: JEOL JEM-ARM200F
- Type of the electron gun: Cold field emission (CFE)
- Acceleration voltage: 200 kV
- Without a monochromator
- Imaging mode: STEM

— Probe diameter in the STEM mode: 0,2 nm

Setup conditions of the EELS are as follows.

— Model of the EELS: Gatan GIF Quantum ER Model 965 (parallel detection)

— Diameter of the entrance aperture: 2,5 mm

A.3.2 First energy step, δE_1 , calibration

A.3.2.1 Determining the EELS first energy step, δE_1

Select energy step δE_1 to set a full measurement range as the zero-loss peak to the carbon K edge E_{C-K} of graphite. E_{C-K} is 284,5 eV. Channel number m of Gatan GIF Quantum ER is 2048. See [Formula \(A.1\)](#):

$$\delta E_1 \geq 284,5 / 2048 = 0,1389 \text{ eV} \quad (\text{A.1})$$

δE_1 should be greater than or equal to 0,1389 eV. The energy step is selected from preset values of Quantum ER. Selected energy step δE_1 is 0,25 eV.

A.3.2.2 Acquisition of carbon K-edge EEL spectrum

Irradiate electron beam to graphite. Acquire EEL spectrum including the zero-loss peak and carbon K edge E_{C-K} of graphite as [Figure A.2](#) and [Figure A.3](#). In this annex, position of the zero-loss peak is expressed as the zeroth channel number.

A.3.2.3 Obtain the value for CH_1 between the zero-loss peak and carbon K edge of graphite

Under the energy step δE_1 , channel number $Ch_1(G, P)$ from the zero-loss peak [[Figure A.2](#), key 1] to plasmon-loss ($\pi + \sigma$) peak [[Figure A.2](#), key 2] and channel number $Ch_1(G, C-K)$ from plasmon-loss ($\pi + \sigma$) peak [[Figure A.3](#), key 2] to the carbon K edge E_{C-K} [[Figure A.3](#), key 3] are obtained. The EELS carbon K edge E_{C-K} position corresponding to the XPS C1s peak is set to half height between peak and dip of background-subtracted spectrum. See [Formula \(A.2\)](#):

$$CH_1 = Ch_1(G, P) + Ch_1(G, C-K) = 106 + 994 = 1100 \quad (\text{A.2})$$

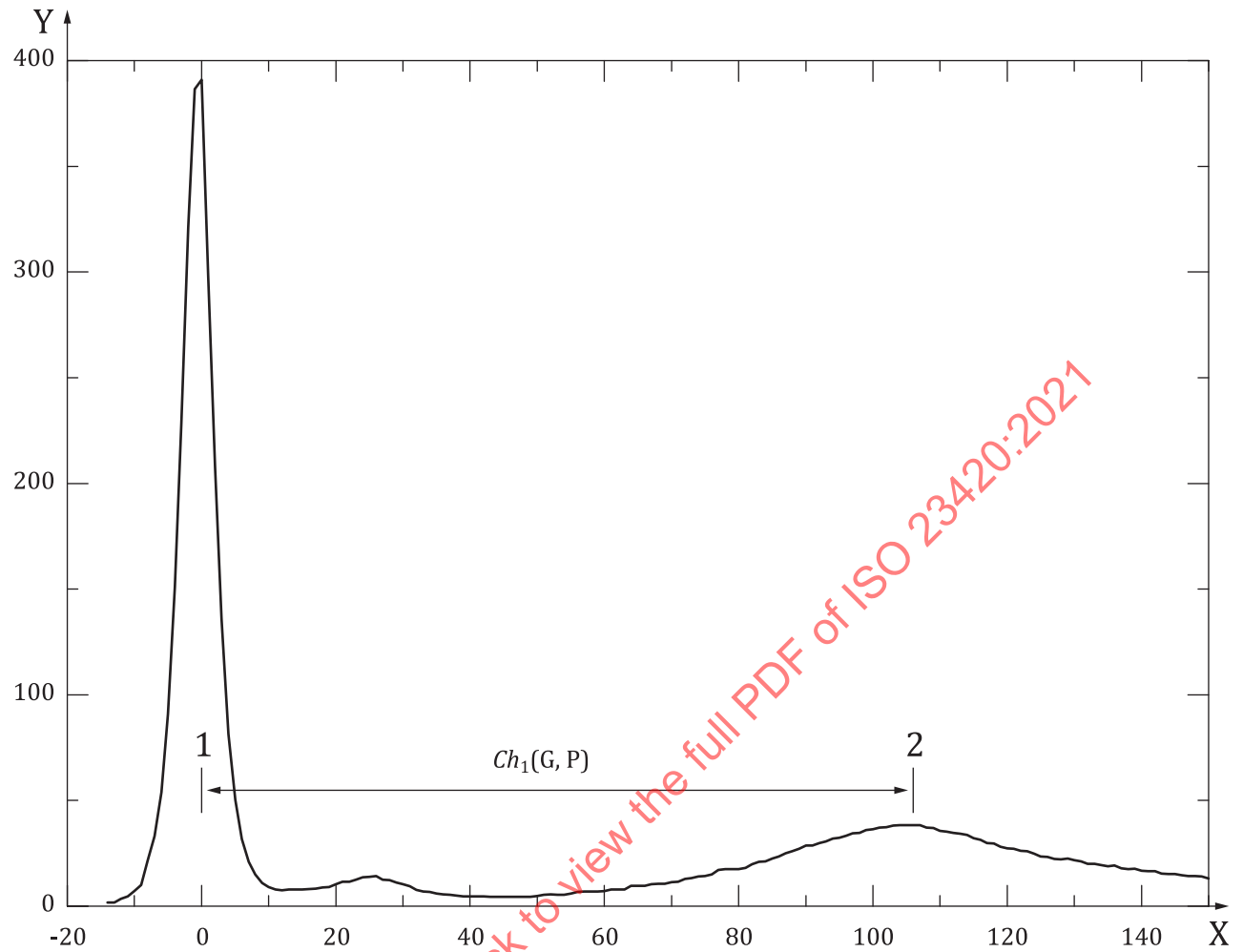
A.3.2.4 Calculate calibrated energy step δE_{1C}

Calibrated (actual) energy step δE_{1C} is obtained under condition of energy step δE_1 (= 0,25 eV). See [Formula \(A.3\)](#):

$$\delta E_{1C} = E_{C-K} / CH_1 = 284,5 / 1100 = 0,2586 \text{ eV} \quad (\text{A.3})$$

Accuracy of coarse energy step is as given in [Formula \(A.4\)](#):

$$(\delta E_1 - \delta E_{1C}) / \delta E_{1C} = (0,25 - 0,2586) / 0,2586 = -0,033 \text{ (-3,3 \%)} \quad (\text{A.4})$$

**Key**

X channel number

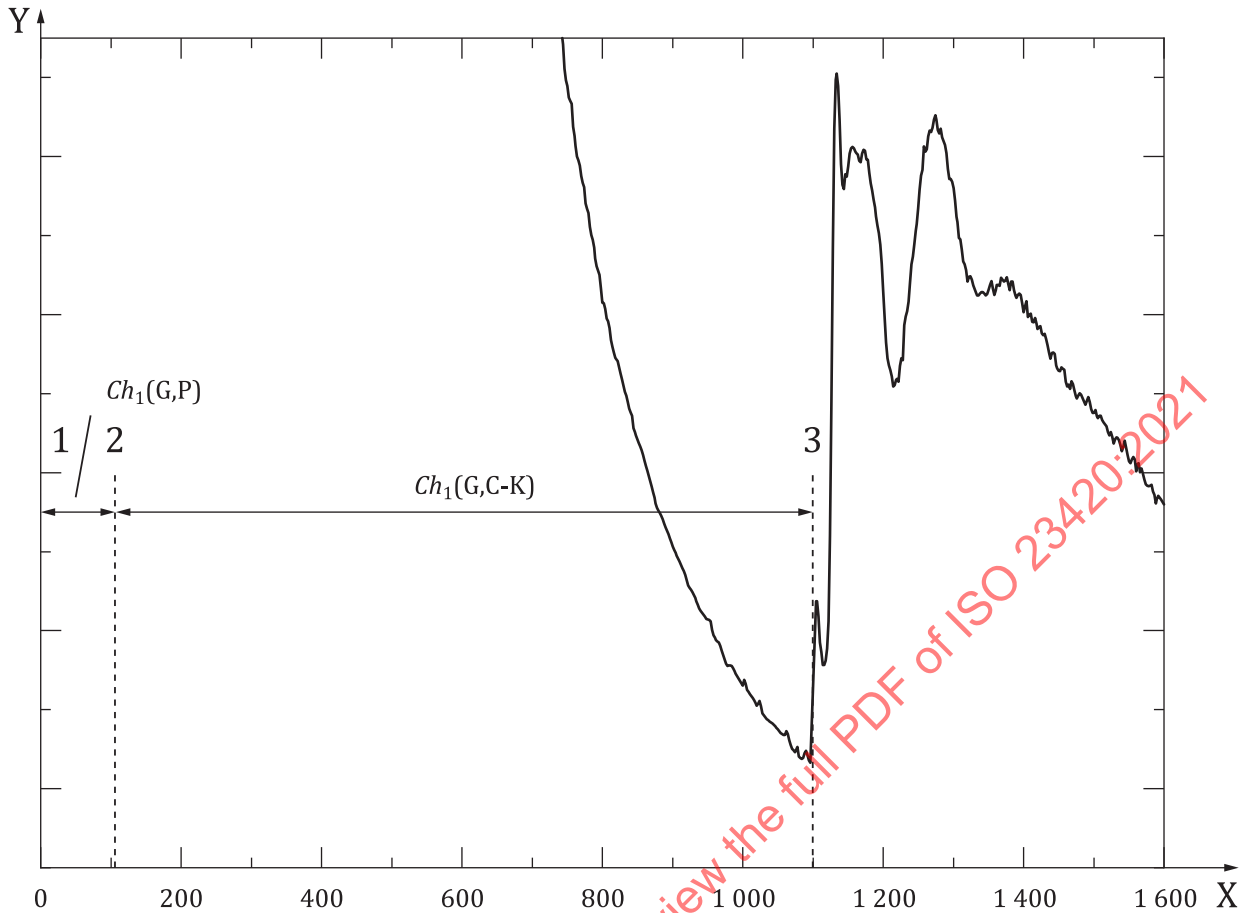
Y counts ($\times 10^6$)

1 zero-loss peak

2 plasmon-loss ($\pi + \sigma$) peak

NOTE Position of the zero-loss peak is expressed as the zeroth channel number.

Figure A.2 — EEL spectrum of the zero-loss peak and plasmon-loss ($\pi + \sigma$) peak for graphite



Key

- X channel number
- Y counts (x10⁴)
- 1 zero-loss peak
NOTE This peak is the same as the key 1 of [Figure A.2](#).
- 2 plasmon-loss ($\pi + \sigma$) peak
NOTE This peak is the same as the key 2 of [Figure A.2](#).
- 3 carbon K edge

Figure A.3 — EEL spectrum of plasmon-loss ($\pi + \sigma$) peak and carbon K edge for graphite

A.3.3 Measurement of peak close to the zero-loss peak, E_{CZLP} , for the other reference sample using energy step δE_1

A.3.3.1 EEL spectrum acquisition of the second reference sample using energy step δE_1

The plasmon-loss ($\pi - \pi^*$) peak of boron-nitride is used as peak E_{CZLP} of the other reference.

Irradiate electron beam to boron-nitride. EEL spectrum including the zero-loss peak and the peak E_{CZLP} has been acquired as [Figure A.4](#).

A.3.3.2 Obtain the value for CH_2 between the zero-loss peak and the peak E_{CZLP}

Channel number CH_2 from the zero-loss peak [[Figure A.4](#), key 1] to peak E_{CZLP} [[Figure A.4](#), key 2] has been obtained. Obtained CH_2 is as given in [Formula \(A.5\)](#):

$$CH_2 = 33 \tag{A.5}$$